

Fe-Cu Compounds in Dye-Sensitized Solar Cells: Influence of Magnetic Field on Mesoporous Structure

Abdul Hai Alami^{a,*}, Di Zhang^a, Camilia Aokal^a, Jihad Abed^b, Ideisan Abu Abdoun^c, Hussain Alawadhi^d

^a Sustainable and Renewable Energy Engineering Department, University of Sharjah, P.O.Box 27272m Sharjah, UAE

^b Masdar Institute of Technology, Abu Dhabi, United Arab Emirates

^c Department of Chemistry, University of Sharjah, P.O.Box 27272m Sharjah, United Arab Emirates

^d Applied Physics Department, University of Sharjah, P.O.Box 27272m Sharjah, United Arab Emirates

Abstract

This paper investigates the effect of applying a static and dynamic magnetic field in the process of depositing the Fe-Cu compound on the working electrode of a dye-sensitized solar cell (DSSC). Depositing this compound on glass is especially hard due to the unfavorable layer inconsistencies that accompany the utilization of the doctor blade technique and the dissociation of the compound at a temperature of 700°C, which prevents its ability to be evaporated or sintered beyond that temperature. The Fe-Cu compound is appreciably cheaper, relatively simple to produce and is more absorptive (>81%) in the Vis-NIR than the standard TiO₂ mesoporous material normally used for DSSCs. The high diffusion of the Fe into the Cu lattice allows the compound to behave as a semiconductor and is found to have a bandgap of 1.8V. The sensitizer used in the production of a test cell consisted of a Schiff base dye with a compatible bandgap of 1.68 eV and resulted in more generated photocurrent than its TiO₂ counterpart, which is a promising result for an alternative mesoporous layer in solar cells.

Keywords: Ferromagnetic Mesoporous Material, Dye-sensitized Solar Cells, Schiff Base Dyes

1. Introduction

Recently, third generation dye sensitized solar cells (DSSC) are seen as a real competitor to conventional silicon based cells and even thin film silicon cells due to their adequate energy conversion efficiency, low cost and ease of manufacturability [1-3].

For even higher energy conversion efficiency values of DSSCs, researchers are improving the performance of individual cell components and, relatable to the work presented here, enhancing the mesoporous nanocrystalline film deposited on the transparent electrode which is known to improve its radiation absorptivity in the UV-Vis ranges on one hand, and enhance the adsorption of dye sensitizers [4-6]. While

titanium dioxide (TiO₂) is the most commonly used mesoporous material, a cheaper, recyclable and more optically absorptive alternative is sought, some of which include integrated schiff bases where they are able to achieve large surface areas and efficient electron transfer [7-12]. Another example is to replace it with a mechanically alloyed p-type Fe-Cu compound semiconductor that is found to enhance the UV-Vis absorptivity to 81% compared to that of TiO₂ [13]. One challenge is to effectively deposit it on the transparent electrode, as heating the Fe-Cu compound above 700 °C causes its dissociation. By taking advantage of the iron content of the compound, the effects of a magnetic field (either static or dynamic) coupled with heating provides a good surface adhesion with the transparent electrode. The effect of magnetic fields has recently gained noticeable attention due to their ability to enhance

* Corresponding author

E-mail: aalalami@sharjah.ac.ae

© 2016 International Association for Sharing Knowledge and Sustainability

DOI: 10.5383/ijtee.11.01.010

performance in applications that range from catalysis to electronics and energy [14]. To influence the photocurrent produced in DSSCs, the generation of charge carriers depends on whether or not the cell has been poled by an external magnetic field [15]. The application of magnetic stirring, mentioned in literature, homogenizes TiO₂ mixtures before depositing them on transparent electrodes [16]. Ferroelectric-photovoltaic devices, in which a homogeneous photoelectric layer is utilized for radiation absorption, have also been investigated although the main materials of choice were ferroelectric oxides and their efficiency was rather low.

There exist a wide selection of dyes to be used as sensitizers in DSSCs, each with different construction and properties, such as natural, organic and synthetic. Conjugated Schiff base polymers and oligomers have been widely studied recently due to some of their outstanding properties that include: thermal, mechanical, optical, optoelectronic, electronic, and fiber-forming properties [17-21].

In this work, we convey the effect of applying static and dynamic magnetic fields on the optical properties and adsorption capacity of the Fe-Cu mesoporous layer, and the impact of any enhancement this has on the performance of the DSSC. The compound is produced using high-energy ball milling where pronounced diffusion of BCC Fe into FCC Cu is achieved. This alters the mechanical, optical and electrical properties of the nano-scale quasicrystalline compound. For best spectral absorptivity and compatible bandgap values with the proposed Fe-Cu mesoporous layer, suitable organic dyes are also tested and selected. We also introduce the thermally stable conjugated Schiff base compound as a dye in the DSSC.

2. Experimental

2.1 Fe-Cu Powder Synthesis by Ball Milling

The process of mechanical alloying is performed using a Retsch PM 100 planetary ball mill with a starting amount of 4.5 g of high purity copper (< 425 µm, 99.5%) and iron (99%) powders, as received from the supplier (Sigma-Aldrich) in a 25 ml stainless steel grinding bowl. The target composition of 50:50 of Fe and Cu (% wt.) is pursued at a controlled milling speed of 400 rpm. The filling ratio within the bowl was needed to be kept at 5:1, this meant that six 10-mm stainless-steel balls are used. Milling is carried out for an hour at a time, pausing after each hour to allow for the collection of a few milligrams of the powder for further characterization and testing and also to cool the equipment. It took thirteen hours for the microstructural changes to become small changes, after which the run is terminated.

2.2 XRD and EDX characterization

To provide information on the composition and grain structure of the developing solid solution, X-ray diffraction (XRD) patterns are plotted for collected powder samples at two-hour intervals for the length of the experiments. The X-ray patterns are recorded with a Bruker D8 Advance DaVinci multipurpose X-ray diffractometer with Cu K radiation operating at $\lambda = 1.5406 \text{ \AA}$, 40 kV tube voltage and 40 mA current. The lattice parameter was then found using Cohen's method and the grain size by the Full-width half-max (FWHM) analysis with the Hall-Williamson method and Bragg's formula.

2.3 Fe-Cu Deposition on ITO

After the desired microstructure of the single phase FCC(Cu) compound is formed and verified by XRD and EDX, it is deposited on a glass slide over an indium-tin oxide (ITO) conductive layer. This was performed using doctor blading technique, where the Fe-Cu compound, mixed in glycerol, is spread onto four identical ITO glass slides using a glass rod to obtain a homogenous thin film. The deposited film is then sintered using three plate heaters, two of which had magnetic stirring turned on with one glass slide placed at the center of each, while the third plate heater had two of the remaining slides share the central position, hence sharing the same applied static magnetic field. The samples are left on the heaters for thirty minutes at 230-250° C. Then, two slides, one from a stirred magnetic field effect and the other from a static magnetic field effect, were used to manufacture the DSSC. The remaining had their powders transferred onto carbon tape for absorptivity and SEM analysis.

2.4 SEM Micrographs

A scanning electron microscope (SEM) and the coupled energy dispersive X-ray spectrometer (EDX) are used to examine fused pieces of the material collected after thirteen hours of milling time. The SEM is a VEGA3 XM by TESCAN, operating at 5 kV, while the EDX analysis is conducted with both map and point modes at the same operating voltage; the former was acquired during 3 minutes while the latter was from four different spots of the sample during 30s live time.

2.5 Optical Properties (Absorptivity)

After 13 hours of milling, spectral measurements of absorption in the ultraviolet, visible and near-infrared (UV-Vis-NIR) regions were carried out on the powders within an integrating sphere attached to two Maya 2000-Pro high-resolution spectrometers (OceanOptics). One dedicated for the UV wavelength range (200-380 nm), and the other dedicated to the Vis-NIR range (375-850 nm), both having a resolution of 0.2 nm and 300 lines per mm diffraction gratings and 10-µm entrance slit. The

signals are transported via a fiber optic cable 2-m long, and of a 200- μm -core diameter. The integrating sphere (OceanOptics ISP-REF, with a sample aperture of 0.4 inch) has a built-in tungsten halogen light source (Ocean Optics LS-1-LL) and is capable of measuring specular and diffuse reflectance. A reference surface in the form of a reflection standard (B0071519) is used to store baseline absorbance (0%) spectra to facilitate comparison between the various compositions.

2.6 Solar Cell Manufacturing and Testing

Two cells were constructed with each Fe-Cu compound variations deposited on the photoelectrode to quantify the effects of magnetic patterning of the Fe-Cu on its effectiveness as a mesoporous material in DSSCs. A homogenous paste was prepared from the two compounds and then spread as a thin layer by employing the doctor blading technique on ITO coated glass (15 – 25 μm /sq., used as received from Sigma-Aldrich) as outlined in section 2.3. The electrolyte used is the I^-/I_3^- classic redox electrolyte prepared from 127 mg iodine crystals, 830 mg potassium iodide and 10 ml ethylene glycol which are mixed thoroughly until completely dissolved. The electrolyte will be the diffusion medium for ionic species between the working photoelectrode prepared as above and the counter electrode made up of a pure copper sheet (99.5% copper sheet 1.2 mm thickness, used as received from Sigma-Aldrich) with carbon deposits on an area of 2.5 x 2.5 cm to enhance the surface area and consequently the conductivity. The injection of electrons and diffusion of ionic species, or the operation mechanism, of DSSCs is well explained and documented in literature for the I^-/I_3^- redox electrolyte [40]. The testing of the solar cell to measure its power conversion efficiency (PCE), fill factor (FF) and IV characteristics are conducted using a solar simulator Xenon Arc Lamps setup, capable of providing irradiance between 0.1-1 suns (up to 1367 W/m^2). The setup was used to provide a constant irradiation on the cells, and was kept at a vertical distance of 30 cm at 1.5 AM and 25 $^\circ\text{C}$. The cell characterization is conducted using VSP-300 potentiostat from Biologic with a potential resolution of 1 μV and a control voltage of ± 10 V up to ± 48 V. The voltage was varied at a rate of 10 mV/s and the current was recorded at each point until the measured voltage reached the open circuit voltage, V_{OC} .

3. Results and Discussion

3.1 XRD and EDS characterization of the Milled Powder

The desired quasicrystalline phase was formed after thirteen hours of ball milling, as confirmed by the XRD analysis of Figure 1 (a), and the resulting grain size is shown in Figure 1 (b), showing a nominal size of around 10 nm.

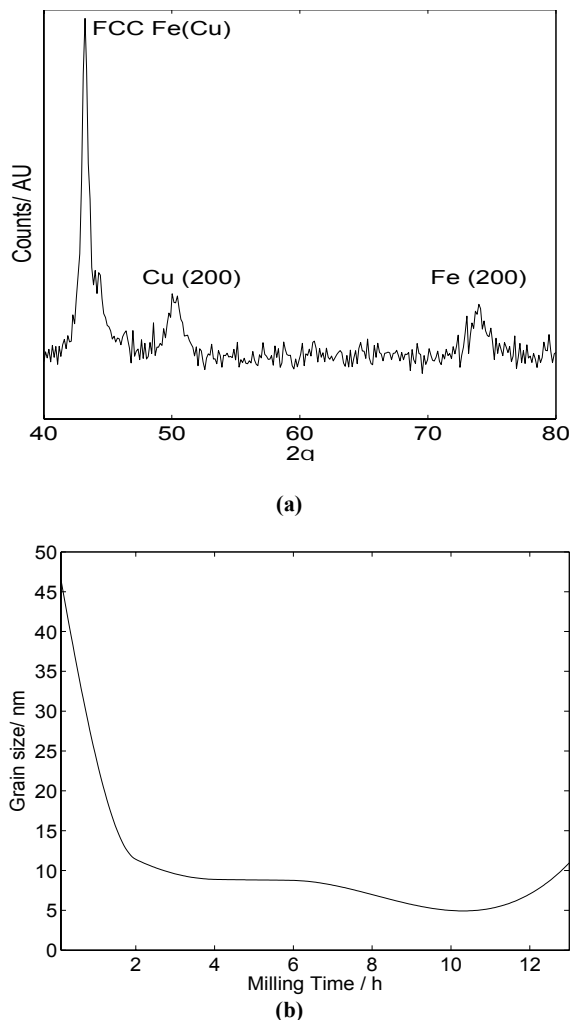


Fig.1. (a) XRD Plot of the Fe-Cu Compound and (b) the Resulting Grain Size

3.2 Fe-Cu Deposition on ITO and SEM Image

Clear differences between the resulting patterns are seen in Figure 2 when comparing the SEM images of Fe-Cu compounds deposited on ITO glass with and without magnetic stirring. A rougher surface is visible in the magnetically stirred sample due to the radial motion of the grains in response to the applied rotating magnetic field. Specimens subject to the static magnetic field show a clustering of the grains, while others under the dynamic magnetic field exhibit an apparent shift of these grains where significant agglomeration is seen, which increased the layer thickness during the radial motion of the particles in response to magnetic stirring.

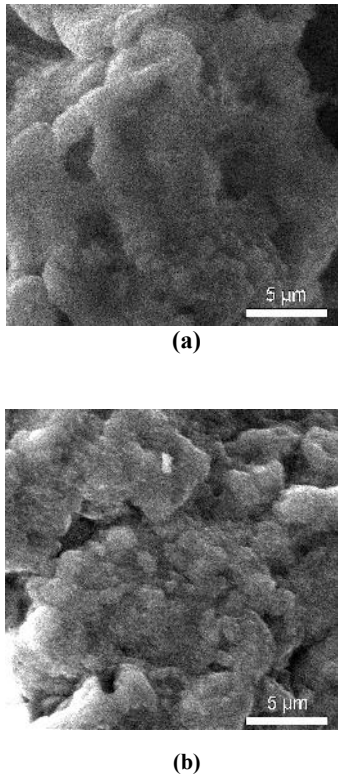


Fig. 2. SEM Micrographs for Fe-Cu Structure at 10kx Magnification (a) with Static Magnetic Field and (b) with Magnetic Stirring

During the sintering/stirring process and whenever magnetic stirring is present, a visual inspection of the resulting layer reveals the presence of concentric circles, as seen in Figure 3 (b).

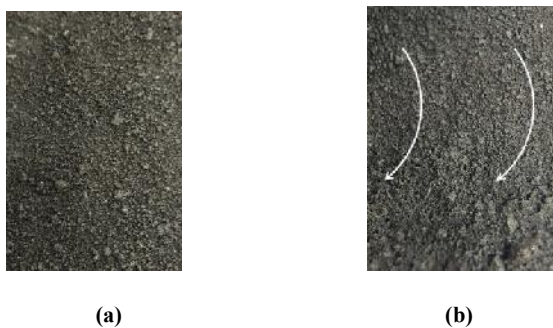


Fig. 3. Micrographs for Fe-Cu Structure (a) without Magnetic Stirring and (b) with Magnetic Stirring, Showing a Concentric Circles Pattern

3.3 Optical Absorptivity of Fe-Cu Compound

The figures below show the optical absorptivity results where Figure 4 (a) and (b) account for the UV and Vis-NIR ranges, respectively. A behavior similar to that of TiO₂ in the UV range although the absorptivity peak is shifted from around 350 nm to around 410 nm as seen in Figure 4 (a).

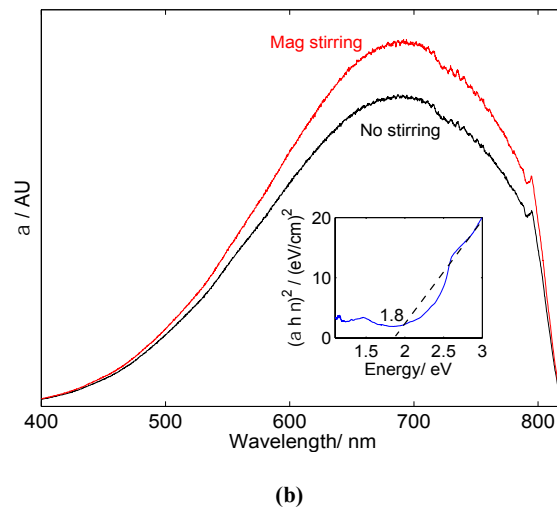
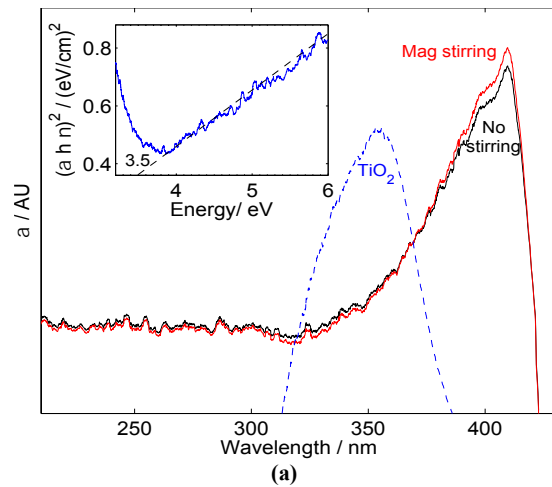


Fig. 4. The Optical Absorptivity shown For two Specimens of Fe-Cu compound, one magnetically stirred while being heated and another only heated in the (a) UV range and (b) Vis-NIR ranges with the optical bandgap (inset)

The absorptivity is then observed to grow steadily in the Vis-NIR ranges to reach a peak at around 680 nm for both specimens of magnetic and non-magnetic stirring effects, as shown in Figure 4 (b). The magnetic stirring shows stronger absorption magnitudes at the edge of the visible region, where the area under the absorptivity curve is 15% larger than that without stirring, indicating an enhancement in absorptivity due mainly to the alterations observed in the microstructure, and seen in the SEM graphs of Figure 2.

Given the shape of the absorptivity, the bandgap of the compound is of interest to be calculated, and thus the absorptivity results were substituted into Tauc equation and the resulting intercept with the abscissa, which gives the bandgap energy is found to be 1.8 eV in the Vis-NIR range, which is a value consistent with ones found for the compound in previous investigations [13] and shows good compatibility with the Schiff base dye used.

3.5 Characterization of the Solar Cell

The employed Fe-Cu (with static magnetic field) and TiO₂ working photoelectrodes on DSSCs were fabricated and characterized side-by-side. Nevertheless, a relatively fast degradation of the device was observed even though the measurement was performed immediately after cell assembly. Insufficient adhesion of the Fe-Cu film sample to the ITO substrate by magnetic stirring was found to be insufficient for cell assembly. The degradation in DSSC may be due to the electrolyte degrading or the fast desorbing of the dye from the working electrode [22]. As a result, partial current density-voltage (J-V) characteristics for both cells were obtained. From Figure 5 that shows the extrapolated I-V characteristics, it can be seen that the Fe-Cu DSSC demonstrated a much larger short-circuit current density of 0.052 mA/cm², compared to that of ~0.002 mA/cm² of TiO₂ device. The significantly increased photocurrent of the Fe-Cu can be attributed to both the unique property of Fe-Cu material and the magnetic field effect: with the static magnetic field, the Fe-Cu layer can be aligned in a single direction (pointing away from the substrate plane), forming a more ordered microstructure which is beneficial for dye absorption; furthermore, the Fe-Cu with increased roughness shows higher absorptivity than TiO₂ in the visible region, as shown in Fig. 4 (b), which can contribute to the light trapping of the attached dye for photocurrent generation. Differently, the open-circuit voltage (V_{OC}) of Fe-Cu is only ~0.018 V, which is approximately an order smaller than the reference TiO₂ device (0.26 V). The considerable loss in V_{OC} may arise from the much larger contact resistance of the Fe-Cu electrode (with a larger thickness) than TiO₂. Consequently, more precise control on the thickness of the layer by a different deposition method is highly preferable for further applications of the Fe-Cu material.

4. Conclusion

In this work, an investigation was carried out on the influence of a magnetic field on the production of a homogenous mesoporous layer made of the Fe-Cu quasicrystalline compound by testing its spectral absorption and its performance in a dye-sensitized solar cell. The bandgap of this compound, which exhibits semiconducting performance, was calculated from absorptivity results to be 1.8 eV. A homogenous layer with excellent light absorption characteristics in the Vis-NIR ranges resulted from the magnetic field applied that was used to assist in the proper arrangement of the compound on the transparent electrode throughout the deposition process. The Schiff base sensitizing dye used was chosen because it has a compatible bandgap of 1.68 eV, and the assembled cell gave a current density of around 0.05 mA/cm² although its open circuit voltage was around 0.02 V. A high throughput process of mechanical alloying in a ball mill was used to make the Fe-Cu nano-scale homogenous compound, which has a potential to replace TiO₂ as a cheaper, recyclable mesoporous layer with better light harvesting characteristics.

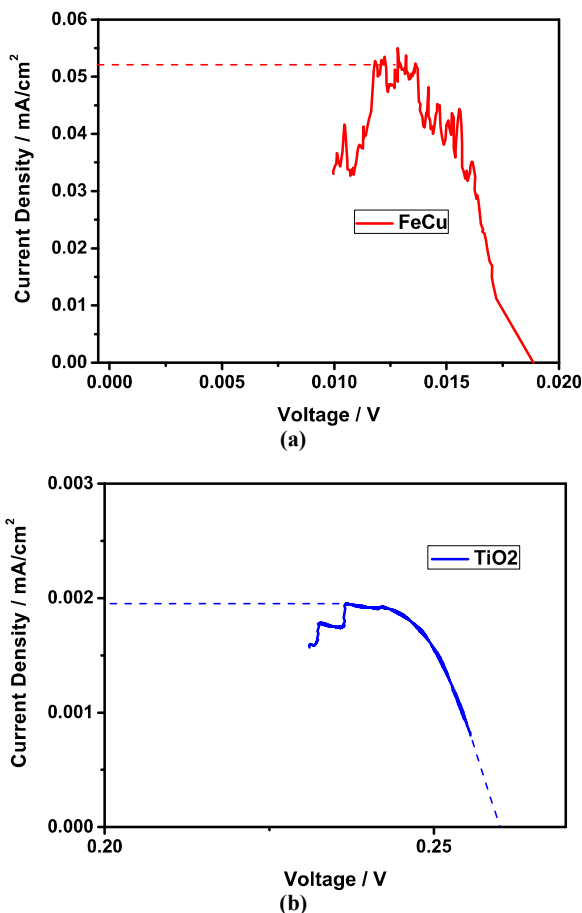


Fig. 5. Characteristic Curves for the (a) Fe-Cu Based Cell (with Static Magnetic Field) and (b) TiO₂ Based Cell

References

- [1] O'Regan B, Grätzel M. A low-cost, high-efficiency solar cell based on dye-sensitized colloidal TiO₂ films. *Nature*. 1991;353(6346):737-740.
- [2] Nazeeruddin M, Péchy P, Grätzel M. Efficient panchromatic sensitization of nanocrystalline TiO₂ films by a black dye based on a trithiocyanato-ruthenium complex. *Chemical Communications*. 1997;(18):1705-1706.
- [3] Green M, Emery K, Hishikawa Y, Warta W, Dunlop E. Solar cell efficiency tables (version 46). *Prog Photovolt: Res Appl*. 2015;23(7):805-812.
- [4] Yella A, Lee H, Tsao H, Yi C, Chandiran A, Nazeeruddin M et al. Porphyrin-Sensitized Solar Cells with Cobalt (II/III)-Based Redox Electrolyte Exceed 12 Percent Efficiency. *Science*. 2011;334(6056):629-634.

- [5] Chiba Y, Islam A, Watanabe Y, Komiya R, Koide N, Han L. Dye-Sensitized Solar Cells with Conversion Efficiency of 11.1%. *Jpn J Appl Phys.* 2006;45(No. 25):L638-L640.
- [6] Wang L, Shi Y, Zhang H, Bai X, Wang Y, Ma T. Iron oxide nanostructures as highly efficient heterogeneous catalysts for mesoscopic photovoltaics. *J Mater Chem A.* 2014;2(37):15279.
- [7] Aegerter M, Schmitt M, Guo Y. Sol-gel niobium pentoxide coatings: Applications to photovoltaic energy conversion and electrochromism. *International Journal of Photoenergy.* 2002;4(1):1-10.
- [8] Bakhshayesh A, Bakhshayesh N. Enhanced performance of dye-sensitized solar cells aided by Sr,Cr co-doped TiO₂ xerogel films made of uniform spheres. *Journal of Colloid and Interface Science.* 2015;460:18-28.
- [9] Mir N, Salavati-Niasari M. Preparation of TiO₂ nanoparticles by using tripodal tetraamine ligands as complexing agent via two-step sol-gel method and their application in dye-sensitized solar cells. *Materials Research Bulletin.* 2013;48(4):1660-1667.
- [10] Masjedi M, Mir N, Noori E, Gholami T, Salavati-Niasari M. Effect of Schiff base ligand on the size and the optical properties of TiO₂ nanoparticles. *Superlattices and Microstructures.* 2013;62:30-38.
- [11] Liu J, Wang Y, Sun D. Enhancing the performance of dye-sensitized solar cells by benzoic acid modified TiO₂ nanorod electrode. *Renewable Energy.* 2012;38(1):214-218.
- [12] Navaneethan M, Archana J, Arivanandhan M, Hayakawa Y. Functional properties of amine-passivated ZnO nanostructures and dye-sensitized solar cell characteristics. *Chemical Engineering Journal.* 2012;213:70-77
- [13] Alami A, Alketbi A, Almheiri M. Synthesis and Microstructural and Optical Characterization of Fe-Cu Metastable Alloys for Enhanced Solar Thermal Absorption. *Energy Procedia.* 2015;75:410-416.
- [14] Li F, Xin L, Liu S, Hu B. Direct measurement of the magnetic field effects on carrier mobilities and recombination in tri-(8-hydroxyquinoline)-aluminum based light-emitting diodes. *Appl Phys Lett.* 2010;97(7):073301.
- [15] Cai F, Wang J, Yuan Z, Duan Y. Magnetic-field effect on dye-sensitized ZnO nanorods-based solar cells. *Journal of Power Sources.* 2012;216:269-272.
- [16] Xiao-Hua L, Shu-Qin Y, Yu Z, Zhi-An W, Ning-Kang H. Effects of Different Dispersion Methods on the Microscopical Morphology of TiO₂ Film. *Chinese Physics Letters.* 2007;24(12):3567-3569.
- [17] Grigoras M, Catanescu CO. Imine oligomers and polymer. *J Macromol Sci— Pure Appl Chem Polym C* 2004;44:131–73.
- [18] Jenekhe SA, Yang CJ, Vanherzeele H, Meth JS. Cubic nonlinear optics of polymer thin films. Effects of structure and dispersion on the nonlinear optical properties of aromatic Schiff base polymers. *Chem Matter* 1991;3:985–7.
- [19] Diaz FR, Moreno J, Tagle LH, East GA, Radic D. Synthesis, characterization and electrical properties of polyimines derived from selenophene. *Synth Met* 1999;100:187–94.
- [20] Morgan PW, Kwolek SL, Pletcher TC. Aromatic azomethine polymers and fibers. *Macromolecules* 1987;20:729–39.
- [21] Ragimov AV, Mamedov BA, Gasanova SG. New efficient dielectric and antistatic materials based on oligoaminophenols. *Polym Int* 1997;43:343–6.
- [22] L. Ke, S. B. Dolmanan, L. Shen, P. K. Pallathadk, Z. Zhang, D. M. Y. Lai, H. Liu, Degradation mechanism of ZnO-based dye-sensitized solar cells, *Solar Energy Materials and Solar Cells*, Volume 94, Issue 2, February 2010, Pages 323–326